HHS Public Access

Author manuscript

Allergy. Author manuscript; available in PMC 2024 March 01.

Published in final edited form as:

Allergy. 2023 March ; 78(3): 752–766. doi:10.1111/all.15601.

IgG memory B cells expressing *IL4R* and *FCER2* are associated with atopic diseases

Carlos J. Aranda[*,1,2,9], **Edgar Gonzalez-Kozlova**[*,3], **Sean P. Saunders**[4], **Weslley Fernandes-Braga**[1,2], **Miyo Ota**[1,2,10], **Sriram Narayanan**[5], **Jin-Shu He**[5,11], **Ester Del Duca**[6], **Bose Swaroop**[6], **Sacha Gnjatic**[2,7], **Gail Shattner**[4], **Joan Reibman**[4], **Nicholas A. Soter**[8], **Emma Guttman-Yassky**[6], **Maria A. Curotto de Lafaille**[1,2]

[1]Jaffe Food Allergy Institute, Division of Allergy and Immunology, Department of Pediatrics, Icahn School of Medicine at Mount Sinai (ISMMS), New York, NY, USA

[2]Precision Immunology Institute (PrIISM), ISMMS, New York, NY, USA

[3]Department of Oncological Sciences, ISMMS, New York, NY, USA

[4]Division of Pulmonary, Critical Care, and Sleep Medicine, New York University School of Medicine (NYUSM), New York, NY, USA

[5]Agency for Science, Technology, and Research (A*STAR), Singapore

[6]Department of Dermatology, ISMMS, New York, NY, USA

[7]Tisch Cancer Institute, ISMMS, New York, NY, USA.

[8]Department of Dermatology, NYUSM, New York, NY, USA

Abstract

Background: Atopic diseases are characterized by IgE antibody responses that are dependent on cognate CD4 T cell help and T cell-produced IL-4 and IL-13. Current models of IgE cell differentiation point to the role of IgG memory B cells as precursors of pathogenic IgE plasma

Correspondence: Maria Lafaille or Carlos J Aranda, Address correspondence to cjarandaclemente@gmail.com or maria.lafaille@mssm.edu.

[9]Allergy Diseases Research Group, Instituto de Investigación, Biomédica de Málaga, Málaga, Spain

[10]Applied Biomedical Science Institute, San Diego, CA, USA

[11]ANU Centre for Therapeutic Discovery, the Australian National University, Acton, Australia

[*]These authors contributed equally to his work

Statement of contribution: C.J.A. and E.G-K. carried out the experimental work and data analysis of this manuscript. S.P.S. and S.N. performed initial experiments leading to this project. W.F-B. performed in vitro experiments. J.H. generated the Hu40LB cell line. J.R, N.A.S., G.S., and E.G-Y. contributed clinical samples and clinical history of subjects. M.O. and S.G. contributed to critical discussion. C.J.A. and M.A.C.L. designed the study, and C.J.A., E.G-K., and M.A.C.L. wrote the manuscript. All authors read and critically reviewed the manuscript.

Conflict of interest: S.G. reports research funding from Bristol-Myers Squibb, Genentech, Boehringer-Ingelheim, EMD Serono, Takeda, and Regeneron. E.G.Y. has served as a consultant for AbbVie, Amgen, Allergan, Asana Bioscience, Celgene, Concert, Dermira, DS Bio- pharma, Escalier, Galderma, Glenmark, Kyowa Kirin, LEO Pharmaceuticals, Lilly, Mit- subishi Tanabe, Novartis, Pfizer, Regeneron, Sanofi, and Union Therapeutics; a member of advisory boards of Allergan, Asana Bioscience, Celgene, DBV, Dermavant, Dermira, Escalier, Galderma, Glenmark, Kyowa Kirin, LEO Pharma, Lilly, Novartis, Pfizer, Regeneron, and Sanofi; and a recipient of research grants from AbbVie, AnaptysBio, AntibioTx, Asana Bioscience, Boehringer-Ingelheim, Celgene, DBV, Dermavant, DS Biopharma, Galderma, Glenmark, Innovaderm, Janssen Biotech, Kiniska Pharma, LEO Pharmaceuticals, Lilly, Medimmune, Sienna Biopharmaceuticals, Novan, Novartis, Ralexar, Regeneron, Pfizer, UCB, and Union Therapeutics. M.A.C.L. received advisory fees from Genentech. J.R. received consultancy fees from AstraZeneca. Work in this manuscript was funded by NIH grants to M.A.C.L. and was solely carried out at academic institutions (NYU and ISMMS).

cells. The goal of this work was to identify intrinsic features of memory B cells that are associated with IgE production in atopic diseases.

Methods: Peripheral blood B lymphocytes were collected from individuals with physician diagnosed asthma or atopic dermatitis (AD) and from non-atopic individuals. These samples were analyzed by spectral flow cytometry, single cell RNA sequencing (scRNAseq), and in vitro activation assays.

Results: We identified a novel population of IgG memory B cells characterized by the expression of IL-4/IL-13 regulated genes *FCER2*/*CD23*, *IL4R*, *IL13RA1,* and *IGHE*, denoting a history of differentiation during type 2 immune responses. $CD23^{+}IL4R^{+}IgG^{+}$ memory B cells had increased occurrence in individuals with atopic disease. Importantly, the frequency of $CD23^{+}IL4R^{+}IgG^{+}$ memory B cells correlated with levels of circulating IgE. Consistently, in vitro stimulated B cells from atopic individuals generated more IgE^{+} cells than B cells from non-atopic subjects.

Conclusions: These findings suggest that $CD23^{+}IL4R^{+}$ IgG^{+} memory B cells transcribing *IGHE* are potential precursors of IgE plasma cells and are linked to pathogenic IgE production.

GRAPHICAL ABSTRACT

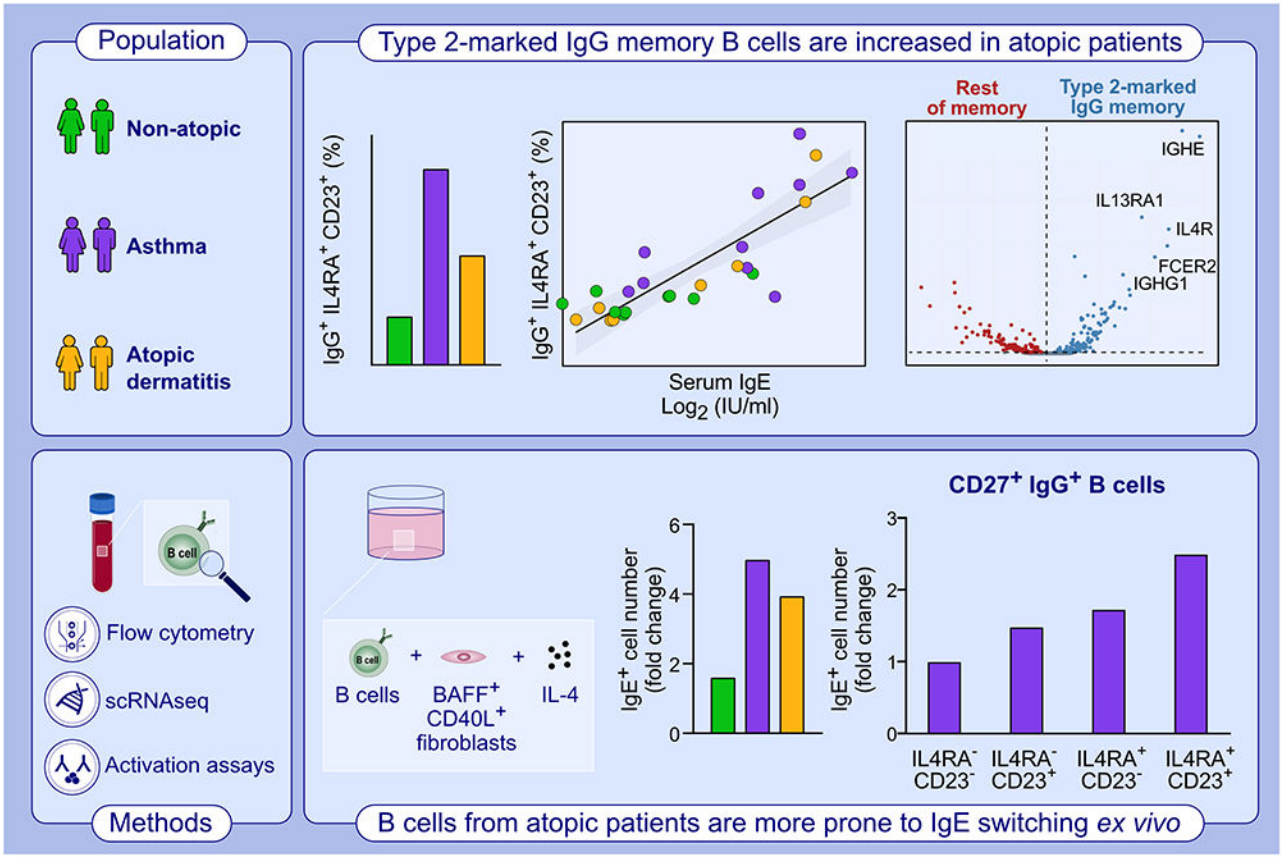

We identified a novel population of IgG+IL4R+CD23+ type 2-marked memory B cells that are increased in peripheral blood of subjects with asthma or atopic dermatitis compared to non-atopic subjects. Type 2-marked IgG memory B cell frequency correlates with circulating levels of IgE antibodies. They express IL-4/IL-13 regulated genes, ie. *FCER2/CD23*, *IL4R*, *IL13RA1* and

IGHE. B cells from atopic subjects generate more IgE cells when stimulated in ex vivo cultures than B cells from non-atopic subjects. IgG+IL4R+CD23+ have the highest ability to switch to IgE among IgG memory B cells.

Keywords

atopic diseases; high-dimensional flow cytometry; IgE; Memory IgG; single-cell sequencing

1. INTRODUCTION

IgE antibodies play a central role in allergic reactions due to their ability to bind to high-affinity FcεR1 receptors on mast cells and induce degranulation upon antigen cross-linking[1,2]. IgE may also contribute to the pathogenesis of chronic allergic inflammation[3]. IgE has the lowest serum concentration and half-life among immunoglobulins[4,5], and IgE-producing B lymphocytes are rare[6,7], yet small amounts of high-affinity IgE can mediate mast-cell degranulation[8,9].

Studies of IgE cell differentiation in mice demonstrated that high-affinity IgE− producing cells form in an unconventional way[10]. Most IgE cells exist as plasma cells, there is a lack of IgE memory cells[11-13], and high affinity IgE plasma cells are generated through the sequential switching of affinity matured IgG1 cells to IgE[11,14-16]. Studies of human atopy support the notion that human pathogenic IgE originates from IgG memory precursors[10]. Sequencing of the switch regions of IgE genes uncovered footprints of the switch regions of IgG1 (Sγ1) and IgG4 (Sγ4)[17], high throughput human BCR repertoire sequencing described relatedness between IgE and IgG repertoires[18,19], and longitudinal studies on allergen specific IgG and IgE antibodies in children found that specific IgG responses precede and are a risk factor for IgE sensitization[10,20,21]. However, unique features of the IgG memory B cells that may be precursors of IgE plasma cells have not been described.

IL-4 and IL-13 are cytokines produced by T cells in type 2 responses that are essential for the development of allergic diseases. IL-4 binds to type I and type II receptors, while IL-13 binds to type II receptors. Type I receptors are formed by the association of IL4Rα with IL2Rγ[22]. The association of IL-13Rα1 with IL4Rα forms the type II receptors[23]. IL-4/IL-13 signaling leads to phosphorylation and nuclear translocation of the transcription factor STAT6. Phospho-STAT6 (pSTAT6) binds to the germline Iε promoter and together with nuclear factor kB (NF-kB), PU.1, and PAX5, induces germline Cε transcription, an essential initial step in class switch recombination (CSR) to IgE[5,24,25]. CSR to IgE also requires simultaneous activation through an activating receptor such as CD40[26,27]. In fact, CD40/CD40L interactions are essential to produce switched antibodies, including IgE in vivo[28]. CD40 signaling activates NF-kB[29], which synergizes with pSTAT6 to activate B cells and induce the enzyme AID, which mediates class switch recombination[30]. In addition, pSTAT6, in conjunction with other transcription factors, activates the promoters of *IL4R*, *FCER2* (encoding CD23), *CD80*, *CD86,* and *MHC II* genes[31], endowing B cells with increased IL-4 responsiveness, increased ability to present antigen to T cells and to undergo CSR to IgE.

The goal of this work was to characterize cell-intrinsic unique features of B lymphocytes from atopic subjects that may be linked to an enhanced ability to switch to IgE. Using flow cytometry and scRNAseq, we identified differences in memory B cell composition between atopic and non-atopic subjects. Importantly, we described a novel population of IgG memory B cells with a type 2-induced profile characterized by expression of IL4R, IL13RA1, CD23, and by transcription of the *IGHE* locus. Type 2-marked IgG memory cells may contain allergen-specific clones and could play an important role in allergy persistence as precursors of IgE plasma cells.

2. MATERIALS AND METHODS

Participant recruitment and blood processing

Atopic and non-atopic subjects were recruited at New York University Medical Center (NYUMC) and Mount Sinai Hospitals (MSH) under protocols approved by the Institutional Review Boards of NYUMC and MSH. Peripheral blood samples were collected in lithium-heparin vacutainer tubes. PBMCs and plasma were isolated by density gradient centrifugation using Ficoll-Paque PLUS (GE Healthcare, Chicago, IL) and cryopreserved in human AB serum (GemCell, Gemini-Bioproducts, West Sacramento, CA) containing 10% DMSO (Sigma-Aldrich, St Louis, MO). PBMCs were stored in liquid nitrogen and plasma samples were stored at - 80°C until use. Participant information can be found in Table S1.

Spectral flow cytometry analysis of B lymphocytes

Cryopreserved PBMCs were thawed and stained for cell-surface proteins by using specific antibodies. Immunoglobulins were stained intracellularly (with exception of IgM and IgD). Cells were analyzed using a Cytek™ 4-laser Aurora (Cytek Biosciences) cytometer. Results were analyzed using FlowJo software (Tree Star Inc., Ashland, OR). Live B cells were gated as $CD19^+$ after the exclusion of dead cells. A full description of sample preparation, data treatment, and analysis are stated in the Appendix S2. Used antibodies are in Table S2.

IgE ELISA

IgE was measured in plasma using a Human IgE ELISA kit from Mabtech (3810-1H) following the manufacturer's directions. Briefly, ELISA plates were coated overnight with anti-human IgE (Clone 107) diluted to 2μg/ml, washed, and then blocked for 1 hour with PBS containing 0.05% Tween 20 and 0.1% BSA. Plasma samples were added, and the plates were incubated for 2 hours at room temperature. After washing, a biotinylated detection anti-human IgE antibody (Clone 182) diluted to 0.3μg/ml was added, plates were incubated for 1 hour at room temperature and washed 5 times. Finally, a 1:1000 diluted streptavidin-HRP was incubated for 1 hour at room temperature, washed 7 times, and color was developed through the TMB procedure (Biolegend 421101). 2N H_2SO_4 was used as a stop solution after 15 minutes.

Cell sorting

Cryopreserved PBMCs were thawed and stained for cell-surface proteins by using specific antibodies for CD19, CD27, IgG, IgD, IgM, CD23, and CD124 (IL4Ra). IgG memory cells were gated as Live-$Dead^-$, $CD19^+$, $CD27^{+/med}$, IgG^+, IgD^-, and IgM^-. 4 different

populations were sorted from the IgG memory compartment based on the expression of CD23 and CD124. Gating strategy and purity check are available as Figure S5C and S5D.

B cell ex vivo expansion

Isolated B cells were seeded over mitomycin-C treated fibroblasts expressing CD40L and BAFF. 10,000 B cells were cultured in the presence of IL-4 (20ng/ml) and/or IL-13 (20ng/ml). Cells were harvested after 8 days. For the sorting experiments, a total number of 1,000 cells of each of the sorted populations were cultured in the presence of IL-4 (40ng/ml) for 8 days. B cells were then stained for flow cytometry extracellularly for CD19, CD27, CD38, IgM, and IgD and intracellularly for IgG, IgA and IgE. Before acquiring the samples, 5ul of CountBright Absolute Counting Beads (Invitrogen C36950) were added to each sample. Cells were acquired in a 4 laser CytoFLEX (Beckman Coulter) cytometer. Results were analyzed using FlowJo software (Tree Star Inc., Ashland, OR).

Single cell RNA sequencing (scRNAseq): library preparation and sequencing

Total B cells were isolated using EasySep™ Human Pan-B Cell Enrichment Kit (StemCell Technologies #19554) from frozen PBMCs. Purified B cells were counted and stained for AbSeq and Multiplexing antibodies following the manufacturer's instruction. Samples were grouped in sets of 4 (1:1:1:1) in 4 different cartridges. Approximately 54000 cells were loaded per cartridge. 3 different libraries (mRNA, AbSeq, and Sample-Tag) were prepared per cartridge following the mRNA Whole Transcriptome Analysis (WTA), AbSeq, and Sample Tag Library Preparation following Protocol Revision 23-21752-00 by BD Biosciences. Libraries were sequenced using an Illumina NovaSeq sequencing S4 by Genewiz LLC. A full description of sample preparation, data quality, data treatment, and statistical analysis are stated in Appendix S1 and S2.

RESULTS

A population of IgG memory B lymphocytes expressing CD23 and IL4R is increased in the blood of atopic subjects

To determine phenotypic differences between B lymphocytes from atopic and non-atopic subjects, we analyzed using spectral cytometry, total B lymphocytes in PBMC from adult subjects with medically diagnosed atopic dermatitis (AD, n=7) or asthma (AS, n=7), and from non-atopic healthy donors (NA, n=8) (Table S1). To resolve B cell populations according to differentiation stage, immunoglobulin isotype expression, and expression of cytokine receptors and activation markers, we designed a flow cytometry panel containing antibodies to HLA-DR, CD19, CD20, CD24, CD27, CD38, IgM, IgD, IgG, IgA, IgE, CD1c, CD29/ITGB1, CXCR3, CD73, CD22, CD72, CD71 (transferrin receptor), and the IL-4/IL-13 regulated receptors CD23/FCER2, IL4RA, and IL13RA1 (Table S2).

The twenty-three flow files generated in a Cytek™ Aurora cytometer were first concatenated after gating out non-B cells. Conventional manual gating was then used to define: a) $IgD^{+}CD27^{-}$ naïve B cells, b) unswitched $IgD^{+}IgM^{+}$ memory B (MBC) cells and plasmablasts/plasma cells (PC), and c) switched $IgM^{-}IgD^{-}$ MBC+PC (Figure S1A).

We used unsupervised FlowSOM analysis of mean fluorescence intensity (MFI) for each marker to identify populations within naïve and MBC+PCs gated cells, and then compared the distribution of B lymphocytes from the three subjects' groups in the populations.

The most significant differences between subjects' groups were found among $IgM^{-}IgD^{-}$ switched MBC+PC populations ($P1^{s}$-$P10^{s}$; Figure 1A-B), of which $P1^{s}$ to $P8^{s}$ were identified as $CD20^{+}$ switched memory B cells, and $P9^{s}$ and $P10^{s}$, containing $CD20^{low}CD27^{hi}CD38^{hi}$ B cells, as IgA^{+} PC and IgG^{+} PC respectively. $P1^{s}$ and $P4^{s}$ were the largest memory populations, containing $CD23^{-}IL4R^{-}$ IgG^{+} ($P1^{s}$) and $CD23^{-}IL4R^{-}$ IgA^{+} ($P4^{s}$) MBC (Figure 1A-B). Of note were populations $P6^{s}$, $P7^{s}$, and $P8^{s}$, containing $IL4R^{+}IgA^{+}$ MBC ($P6^{s}$), $CD23^{+}IgG^{+}$ MBC ($P7^{s}$), and $IL4R^{+}CD23^{+}IgG^{+}$ MBC ($P8^{s}$).

To determine relationships between the populations, we generated a self-organizing map of clusters where associations are depicted as a tree (Figure 1C), into which single marker expression was mapped (Figure S1B). The two main populations containing IgG^{+} and IgA^{+} MBC ($P1^{s}$ and $P4^{s}$, respectively) divided two regions of the tree. Two small clusters of $CD23^{+}IgG^{+}$ $P7^{s}$ cells and $IL4R^{+}CD23^{+}IgG^{+}$ $P8^{s}$ cells branched out from the main IgG^{+} population. The proximity between $P7^{s}$ and $P8^{s}$ indicates relatedness, and the more distal position of $P8^{s}$ suggests higher differentiation (Figure 1C and Figure S1B). Two other branches coming out from the main IgG^{+} tree contained $CXCR3^{+}CD72^{+}IgG^{+}$ cells ($P2^{s}$), and $CD71^{+}IgG^{+}$ cells, both distant to the $CD23^{+}$ populations (Figure 1C and Figure S1B).

To visualize expression at the single cell level, we generated t-SNE plots of the switched B cells displaying all populations (Figure S2A), and expression of individual markers (Figure S2B). $IL4R^{+}$ and $CD23^{+}$ cells were found mostly among IgG^{+} cells both in $CD27^{+}$ and $CD27^{low}$ t-SNE areas, and $CD71^{+}$ cells were outside and among the $CD23^{+}$ and $IL4R^{+}$ IgG areas (Figure S2B). $CXCR3^{+}$ cells in the t-SNE plots did not co-localize with $CD23^{+}$ or $IL4R^{+}$ cells (Figure S2B). This is consistent with the differential regulation of CXCR3 and IL4R/CD23 by IFNγ and IL-4/IL-13[32,33] respectively, and the known counter regulation between IFNγ and IL-4/IL-13 signaling in B cells[34].

The distribution of B cells from non-atopic (NA), AS and AD subjects among the 10 switched populations was then analyzed (Figure S2C). $P7^{s}$ cell frequency was significantly higher in AS (2.8 fold) and AD (3.3 fold) groups than in the non-atopic group (Figure 1D), and $P8^{s}$ was significantly higher in the AS (4.3 fold) than the non-atopic group (Figure 1E). Other smaller populations that tended to have a higher frequency in the atopic samples were $P3^{s}$ and $P5^{s}$, which expressed the activation marker CD71[35]. In contrast, $P1^{s}$, the main $CD23^{-}IL4R^{-}$ IgG population tended to have a lower frequency in atopic subjects (Figure S2C).

To corroborate the differences in frequency of IL-4R and CD23 expressing IgG^{+} MBC between atopic and non-atopic subjects, we also used conventional manual gating (Figure 1F). AS and AD samples had a significantly lower frequency of $IL4R^{-}CD23^{-}IgG^{+}$ cells than NA samples, and AS samples had a significantly higher frequency of $CD23^{+}IgG^{+}$ and $IL4R^{+}CD23^{+}IgG^{+}$ than NA samples (Figure 1G). No significant differences were found for conventionally gated IgA^{+} cells (Figure S2D).

We next analyzed CD27 expression in IL4R$^+$, CD23$^+$, IL4R$^+$CD23$^+$, and IL4R$^-$CD23$^-$ IgG$^+$ MBC and found that most of these cells expressed CD27, with the highest CD27 expression being among the IL4R$^-$CD23$^-$ and CD23$^+$ IgG cells (Figure 1H and Figure S2E). Previously, a population of CD27$^-$IgD$^-$ double negative B cells expressing *FCER2/CD23* and *IL4R* markers was reported, but no CD27$^+$ IgG memory B cells with those features were described[36].

The results above identified IL4R$^+$CD23$^+$IgG$^+$ MBC with increased frequency in individuals with asthma or atopic dermatitis.

IL4R$^+$CD23$^+$ and CD23$^+$ IgG$^+$ MBC frequencies correlate with plasma levels of IgE

A direct correlation between IL4R$^+$CD23$^+$IgG$^+$ MBC and IgE antibodies would be consistent with the role of these cells in IgE generation. We thus determined correlations between the CD23 and IL4R expressing IgG$^+$ populations defined in the unsupervised analysis (Figure 1A) and the conventional gating analysis (Figure 1F), and plasma IgE levels (Figure 2A). Positive correlations were found between IgE and all populations expressing CD23: P7^S, P8^s, and conventionally gated IgG$^+$CD23$^+$ and IL4R$^+$CD23$^+$IgG$^+$ (Figure 2B), while IgG$^+$IL4R$^-$CD23$^-$ and IgG$^+$IL4R$^+$ cells correlated negatively with CD23 expressing cells and with IgE antibodies (Figure 2B-C). All correlations are shown in Figure S3A. These findings strongly suggest that IgG$^+$IL4R$^+$CD23$^+$ and IgG$^+$CD23$^+$ MBC are linked to IgE production.

Effects of atopy on IgM memory and naïve B lymphocytes.

Unsupervised and conventional flow cytometry analysis was also carried out for IgM/D$^+$ MBC+PC and for naïve B cells. The unsupervised analysis of unswitched IgM/D$^+$ MBC+PC cells (Figure 3A-B) identified 5 memory populations (P1^u, P2^u, P3^u, P4^u, and P6^u) and a PC population (P5^u). P3^u, the largest population, contained CD23$^-$IL4R$^-$ unswitched MBC. Three small populations contained CD23$^+$ and IL4R$^+$ cells, P1^u, P2^u, and P4^u. Interestingly, P2^u and P4^u branched out from the main tree, P2^u (CD23$^+$) being more internal and P4^u (IL4R$^+$CD23$^+$) distal in the same branch, similarly to equivalent populations of IgG memory. Here too CXCR3 expressing memory cells (P6^u) were not in proximity of the main CD23$^+$ branch (Figure 3B and t-SNE plots in Figure S4A-B), reflecting the differential induction of CXCR3 by IFNγ, and of CD23 by IL-4/IL-13, and counter regulation between IFNγ and IL-4/IL-13 signaling. While no significant differences among groups were found in the unsupervised analysis of populations (Figure 3C), conventional gating identified a significant reduction in CD23$^-$IL4R$^-$ unswitched IgM/D$^+$ memory population in AS and AD compared to non-atopic samples (Figure 3D-E).

Unsupervised analysis of naïve B cells defined 6 populations (P1^n to P6^n), of which P3^n cells were identified as transitional B cells based on expression CD38 and CD24 (Figure 3F-G). P3^n may contain Breg precursors, which are contained in CD24^{hi}CD38^{hi} immature blood B cells[37,38]. IL-10 producing Bregs were found to be decreased in severe AD patients[37,38]. In our analysis, the average frequency of P3^n cells was lower in AS and AD than in NA subjects, but the differences were not statistically significant. IL4R and CD23 are developmentally expressed in large part of mature naïve B cells, as seen in IL4R$^+$CD23$^+$

P1^{n}, the largest naïve population, and IL4R^{+} P5^{n}, the second largest (Figure 3F-G). P4^{n}, IL4R^{-}CD23^{-} relatively abundant naïve population, was found to be significantly decreased in the AS and AD groups compared to the non-atopic group (Figure 3H). Conventional analysis found a significantly decreased frequency of IL4R^{-}CD23^{-} and an increase in the frequency of IL4R^{+}CD23^{+} naïve B in AS versus non-atopic groups (Figure 3I-J).

In sum, we found a significant reduction in CD23^{-}IL4R^{-} unswitched memory and naïve B cells in atopic subjects, and a significant increase in CD23^{+}IL4R^{+} unswitched memory and naïve B in subjects with asthma compared with non-atopic subjects.

B lymphocytes from atopic subjects have a high propensity to switch to IgE

To determine if B cells from atopic subjects had a higher propensity to switch to IgE, we compared the generation of IgE cells in cultures of purified B lymphocytes from non-atopic healthy subjects (NA; n=9), and from subjects with asthma (AS; n=7) or AD (n=9). Purified B lymphocytes devoid of plasma cells (Figure S5A) were cultured on a layer of fibroblasts expressing human CD40L and BAFF (h40LB), without (media) or with the addition of IL-4, IL-13, or IL-4+IL-13 (Figure 4A). The cells were harvested after 8 days of culture and analyzed by flow cytometry (Figure S5B). Total B cell numbers, a proxy for proliferation, were significantly higher in cultures from AD subjects than in those from non-atopic subjects, and a similar tendency was observed in cultures of AS subjects (Figure 4B). IgE cells were quantified in the cultures by intracellular staining (Figure 4C). Very few IgE^{+} cells were found in cultures without IL-4 or IL-13 but the addition of these cytokines promoted class switching to IgE. Importantly, IL-4 and IL-13 stimulated cultures of atopic subjects had a significantly higher frequency of IgE^{+} cells than cultures from non-atopic subjects (Figure 4D). To confirm the contribution of the IgG memory subsets expressing CD23 and/or IL4R to the generation of IgE cells, we sorted IgG cells from asthma and AD patients based on their expression of IL4R and CD23 (Fig S5C-D) and cultured them over h40LB cells with added IL-4. We observed that IL4R^{+}CD23^{+} IgG B cells generated more IgE cells (2.3 fold) than their IL4R^{-}CD23^{-} counterparts. The number of IgE cells in cultures of IL4R^{-}CD23^{+} and IL4R^{+}CD23^{-} was also higher than in IL4R^{-}CD23^{-} IgG cell cultures (1.4 fold and 1.8 fold respectively) though the differences were not statistically significant (Figure 4E). These results demonstrate enhanced response to activation and class switching to IgE of B cells from atopic than non-atopic subjects, and that IL4R^{+}CD23^{+} IgG memory B cells are involved in this response.

Transcriptional profile of B lymphocytes from atopic and non-atopic subjects

To characterize gene expression signatures associated with atopy, we carried out scRNAseq analysis of total B cells from PBMC of non-allergic (n=5), AS (n=3), and AD (n=3) subjects. We quality-controlled the samples by removing cells with more than 25% mitochondrial gene expression, doublets, and expression outliers with extremely large counts (Figure S6A-D). Using Seurat and Monocle3 analysis we identified 15 B lymphocytes clusters contained in three mega clusters of: a) naïve B cells (N1-N6); b) MBC (M1-M7); c) PC (PC1-PC2) (Figure 5A-C and Figure S6E).

A pseudotime analysis of the clusters with N5 as the earliest differentiation stage, suggests a maturation pathway with directionality through transitional (N5→N4) and naïve cells (N2→N1→N3) (Figure 5B and S Dataset A-B). Two main branches of differentiation of memory cells were identified, M1-M4-M7, and M2-M3 with a branch to M6 (Figure 5B). Seurat::FindMarkers analysis identified differentially expressed genes (DEGs) in each cluster (Figure 5C and S Dataset B). Consistent with the pseudotime analysis, the directional relatedness of the transitional to naïve clusters can be seen in the expression of DEGs *NEIL1*, *TCL1A*, *PCDH9*, *SOX4,* and *HRK* (highest is N5, lower in N4), common DEG between N5, N4 and N2 (*FOSB*, *FOS*), common DEGs between N4 and N2 (*FCER2*, *PLPP5*). Naïve cluster N3 can be distinguished from all the other naïve clusters by having the lowest expression of *FOS*, *FOSB,* and *ZPF36*. A high skewness in the distribution of pseudotime values of the transitional and naïve clusters demonstrates homogeneity in the early transitional N5 cluster, while low skewness indicates high heterogeneity in N4, N2, N1, and N3 (Figure S6F).

Among memory B cells, shared DEGs associated with M1/M4/M7 were *GPR183* (encoding EBI2), *ZFP36*, *RGS2,* and *NR4A2*. While M6 is related to M2 and M3 through *TCF7* and *SCIMP*, M2 and M3 share DEGs *LINC01781* and *MARCKS* (Figure 5D-E and S Dataset C). M3 is uniquely characterized by several Ca2+ binding proteins, M7 by *NEAT*, *FGR*, *FCRL5,* and M4 by high expression of *CD1C* (Figure 5D-E and S Dataset C). The differential expression between M1/M4/M7 and M2/M3/M6 shows enrichment of *IGHM*, *IGHD*, *FOS*, *FOSD*, *FOXP1*, and *CD1C* in the M1/M4/M7, while the M2/M3/M6 path is enriched in switched *IGHA*, *IGHG*s, *TCF7*, *COCH* (Figure 5D-E and S Dataset C). The directionality of differentiation and characteristic DEGs are shown in Figure 5E. The low skewness of pseudotime distribution in M1 and M4 indicates heterogeneous cell populations, while high pseudotime skewness in M3, M6, and M7 indicates quite homogenous cell populations (Figure S6G).

Two clusters of PCs were defined (PC1 and PC2), PC1 comprised most IgA (*IGHA*) PC and all IgM (*IGHM*) PC, while PC2 comprised most IgG (*IGHG1/2/3/4*) PC (Figure 5A and Figure S7A-C). The frequency of PC was higher in AD samples than in AS or NA samples, with a particularly high frequency of IgA PC (Figure S7D-E). There were 7 IgE PCs identified, 6 in PC1, and one in PC2 (Figure 6A). All IgE PC were from atopic subjects, 6 from AD and 1 from AS. Differential expression between 7 IgE PC and other cells is possible (Figure S7C and S Dataset D), however, this comparison although significant ($P<0.05$) is underpowered due to the low number of IgE PCs[39].

In sum, we identified naïve, memory, and plasma cell populations in human PBMC, and possible differentiation relatedness and progression were characterized. Notable, two differentiation memory branches were distinguished, one enriched in switched memory B cells and characterized by expression of *TCF7*, a transcription factor associated with self-renewal.

A B cell memory cluster with type 2 immune marks is expanded in atopic subjects

A more in-depth analysis of memory clusters as defined in Figure 5A was performed to identify cluster-specific DEGs and to determine the distribution of cells from atopic and

non-atopic samples in the clusters (Figure 6A). Isotype expression analysis (Figure 6B) showed that M1 and M4 contained predominantly *IGHM*$^{+}$/*IGHD*$^{+}$ cells, M7 contained *IGHD*$^{+}$ and *IGHG3*$^{+}$ cells, and M2 and M3 were enriched in *IGHA1*$^{+}$ and *IGHA2*$^{+}$ cells. M6 was enriched in *IGHG1*$^{+}$ cells and was distinctively the only cluster with significant expression of *IGHG4* and *IGHE*.

Top M6 DEGs were associated with the IL-4/IL-13 pathway, such as *IGHE*, *IL13RA1*, *IL4R*, *IGHG4*, *FCER2,* and *IGHG1* while lacking expression of IFNγ regulated *TBX21* (Figure 6C, Figure S8A-D, and S Dataset E). As most *IGHE* transcribing cells are found in cluster M6 (Figure S8A), which contains *IGHG1*$^{+}$ and *IGHG4*$^{+}$ cells (Figure 6B), these *IGHE*$^{+}$ cells are likely IgG1 or IgG4 MBC transcribing germline *IGHE*. Other genes strongly associated with this cluster are *HOPX*, encoding a transcriptional regulator involved in the persistence of Th1 cells[40], *RNGTT*, encoding an mRNA capping enzyme[41], various MHC II genes and genes related to MHC II antigen presentation and function such as *SCIMP* (SLP adaptor and CSK interacting membrane protein), encoding a transmembrane adaptor involved in MHC II signaling and immune synapse [42] and *CD74*, encoding the invariant chain[43] (Figure 6C-D and S Dataset E).

Importantly, M6 was clearly enriched in cells from atopic donors (AS and AD), and to a lesser extent so did cluster M3 (Figure 6E). In contrast non-atopic (NA) donors' cells were more frequent in clusters M1, M4, and M7 (Figure 6E). A correlation between the LogFC of the top 10 DEG and disease status (Figure 6F) demonstrated a highly significant positive correlation for M6 in the AS vs HC and AD vs HC comparisons, and to a lesser degree for M3. On the other hand, the correlation was negative for LogFC of M1, M4, and M7 DEG in the AS vs HC and AD vs HC comparisons. This comparison also shows a strong association of M5 with AD samples.

Pathway analysis of DEGs from M6 identified GO biological processes associated with positive regulation of proliferation (GO:0050671; GO:0032946; GO:0070665), regulation of size, cytoskeleton, and cell migration (GO:0032535; GO:0008064; GO:0007010; GO:0030334); positive regulation of transcription from RNA polymerase II promoter (GO:0045944), cytokine-mediated signaling pathway (GO:0019221); negative regulation of signal transduction (GO:1902532); regulation of I-kappaB kinase/NF-kappaB signaling (GO:0043122) (Table S3 and S Dataset F). The analysis supports the notion that cells in the M6 cluster are prone to activation and respond to cytokines IL-4 and IL-13.

To determine if active IL-4/IL-13 signaling was necessary for the maintenance of 'type2-marked' memory B cells, we compared the composition of circulating memory B cells from AD donors that were not treated (AD) or were treated with the anti-IL4R blocking antibody dupilumab (DUP). Seurat cluster analysis of 3 AD and 4 DUP samples defined 11 memory clusters (Figure S9A), among them cluster M7' with similar DEGs to the previously described 'type2-marked' M6 cluster in Figure 5-6 (Figure S9B). While the frequency of memory B cells in the type2-marked M7' cluster was on average lower in DUP than AD samples (Figure S9C), type2-marked memory B cells remained present in DUP patients. Remarkably, no IgE PC were found in DUP B lymphocyte samples. This suggests that the atopic signature of B cells is quite resilient once established, perhaps not requiring

active IL-4/IL-13 signaling for maintenance, but IL-4/IL-13 signaling is necessary for CSR to IgE and formation of new IgE PC.

DISCUSSION

In this manuscript, we identified a subpopulation of human IgG memory B cells that express a B cell signature characterized by expression of *FCER2*/CD23, *IL4R*, *IL13RA1,* and *IGHE*, all known targets of IL-4/IL-13 signaling in B cells[44-47]. We referred to these cells as type2-marked IgG memory cells. The frequency of type2-marked IgG memory B cells was higher in individuals with asthma or atopic dermatitis than in non-atopic healthy subjects, and their frequency correlated positively with levels of IgE antibodies in plasma. These findings suggest a common developmental relationship between type2-marked IgG memory B cells and IgE antibodies.

The transcriptional profile of type2-marked IgG memory cells predicts that these cells are well equipped for antigen presentation to T cells and to engage in T-B cell interactions. DEGs of type2-marked IgG memory B cells include MHC II genes, and genes encoding proteins related to MHC II-mediated antigen presentation and signaling, such as the transactivator CIITA, the peptide loading chaperone *CD74*[43], and the transmembrane adaptor *SCIMP*[42].

Differential expression of *IL4R* and *IL13RA1* in type2-marked IgG memory cells predict that these cells would be highly responsive to IL-4/IL-13 signaling, and germline transcription of *IGHE* locus, an essential step for class switching, indicates a readiness to undergo CSR to IgE. Expression of higher levels of *CD40* in type2-marked IgG population is also relevant, as B-T cell interactions through CD40/CD40L and IL4R signaling in B cells are essential for CSR to IgE in vivo[26,48]. The profile of type2-marked IgG memory B cells is thus highly consistent with B cells that can engage in cognate interaction with Tfh cells producing IL-4/IL-13[49] and undergoing CSR to give rise to IgE plasma cells.

Previous studies on the differentiation of IgE cells demonstrated that antigen-specific high affinity IgE plasma cells are formed from IgG memory cells[10,14]. The potential role of type2-marked IgG memory B cells as precursors of IgE plasma cells suggests that this population may contain allergen-specific clones responsible for the long-term persistence of IgE-mediated allergies.

Among memory B cells analyzed by scRNAseq, we identified a *FCER2*$^+$*IL4R*$^+$ memory cluster composed of *IGHG1*$^+$ and *IGHG4*$^+$ positive cells co-expressing *IGHE*, likely reflecting the production of the germline *IGHE* transcript in IgG1 and IgG4 memory cells. Importantly, *IGHG*$^+$*FCER2*$^+$*IL4R*$^+$*IGHE*$^+$ memory B cells identified through scRNAseq clearly corresponded to the IgG$^+$IL4R$^+$CD23$^+$ population identified by flow cytometry. In both types of analysis, we found an increased frequency of this population in atopic patients.

Pseudotime analysis of the scRNAseq data identified two branches of memory B cells, one of them characterized among other genes by expression of Inc-RNA *MIAT*, *RNGTT*, and *TCF7,* which encodes the transcription factor TCF1. The *TCF7* memory branch contained mostly switched memory B cells (*IGHA*$^+$ and *IGHG*$^+$), including the *IGHG*$^+$ *IL4R*$^+$

FCER2^{+} memory cluster. The second memory branch was characterized by a high frequency of *IGHM/IGHD*$^{+}$ expressing cells and by differential expression of *ZFP36*, *GPR183*, *FOS*, and *FOSB* (*ZFP36* memory branch). The *ZFP36* branch contained cells with high *CD1C* expression, and a small cluster of cells expressing *ITGAX*$^{+}$ (encoding CD11c), *FCRL5*, *TBX21* (encoding T-bet), and with low expression of *CR2* (encoding CD21). CD11c^{+}T-bet^{+}CD21^{low} memory B cells are induced by IFNγ during type1 responses[50-52] and have been associated with autoimmunity, aging, and viral immunity[53-56]. Interestingly, memory B cells from atopic subjects tended to be overrepresented in the *TCF7* memory branch, and under-represented in the *ZFP36* memory branch, indicating a propensity to the higher frequency of switched memory B cells in atopic subjects.

Unswitched memory CD23^{-}IL4R^{-} memory B cells had a small but significant decrease in frequency in atopic subjects, which implies an increase in the corresponding CD23 and IL4R expressing cells. Typically, IgM memory B cells carry less somatic mutations than IgG memory cells[57,58], thus IgE derived from direct switching of IgM memory cells would likely be of low affinity, and could modulate the pathogenicity of high affinity IgE[14].

While most memory B cells do not express CD23 or IL4R, these molecules are found in a quite high percentage of the mature naïve B cells. Our results indicate that there is further upregulation of CD23 and IL4R in naïve B cells of atopic subjects. This may represent a risk to produce IgE against novel antigens in atopic subjects.

The scRNAseq studies found few IgE plasma cells from atopic donors among a few hundred total plasma cells. Due to their low number, it was not possible to faithfully identify markers for IgE plasma cells. Nevertheless, IgE plasma cells appear to express a less differentiated PC program as indicated for example by higher expression of *FCER2* and MHC II genes, consistent with the previous observations[7].

It is not known if the stability of the type2-marked IgG memory B cell phenotype requires frequent IL4R signaling. IL4R signaling and CSR to IgE are inhibited by anti-IL4R blocking antibodies[59,60]. However, we found that type2-marked IgG memory cells were still detectable in PBMC samples from four AD subjects treated with anti-IL4R antibody dupilumab, though they were at a reduced frequency in two of the four subjects. Consistent with the described reduction of circulating IgE on dupilumab treatment[61-63], no IgE plasma cells were found in the samples from dupilumab-treated subjects. Though limited, the findings suggest that the B cell type2 signature remains in the absence of or with very reduced IL4R signaling.

In this manuscript, we described a novel population of CD23^{+}IL4R^{+} IgG memory B cells, referred to as type2-marked IgG memory B cells, that differentially express IL-4/IL-13 regulated genes and are found at increased frequency in peripheral blood of atopic subjects. These cells have an expression profile that predicts facilitated CSR to IgE and antigen presentation to CD4 T cells. We hypothesize that the type2-marked IgG cells may contain allergen-specific clones with enhanced ability to differentiate into IgE plasma cells, thus contributing to the long-term persistence of allergy.

This study has limitations due to the restricted number of patients from whom we were able to obtain blood samples, the rather heterogenous nature of the cohorts of atopic and non-atopic subjects analyzed, and the lack of longitudinal samples from dupilumab-treated patients.

Supplementary Material

Refer to Web version on PubMed Central for supplementary material.

Acknowledgments:

We thank Juan Lafaille for critically reading the manuscript. We thank members of the Human Immune Monitoring Center, Genomics, and Flow Cytometry Cores at ISMMS. C.J.A. received a postdoctoral fellowship from the Fundación Areces, Spain. S.P.S was a recipient of the NYU Bernard Levine postdoctoral fellowship. S.G. was supported by grants CA224319, DK124165, and CA196521. S.G. reports research funding from Bristol-Myers Squibb, Genentech, Boehringer-Ingelheim, EMD Serono, Takeda, and Regeneron. Work in the M.A.C.L. laboratory was supported by NIH grants R21AI133076, R01AI151707, and R01AI153708.

REFERENCES

1. Galli SJ, Tsai M. IgE and mast cells in allergic disease. Nat Med. 2012;18(5):693–704. [PubMed: 22561833]
2. Kinet JP. The high-affinity IgE receptor (Fc epsilon RI): from physiology to pathology. Annu Rev Immunol. 1999;17:931–972. [PubMed: 10358778]
3. Logsdon SL, Oettgen HC. Anti-IgE therapy: clinical utility and mechanistic insights. Current topics in microbiology and immunology. 2015;388:39–61. [PubMed: 25553794]
4. Vieira P, Rajewsky K. The half-lives of serum immunoglobulins in adult mice. Eur J Immunol. 1988;18(2):313–316. [PubMed: 3350037]
5. Geha RS, Jabara HH, Brodeur SR. The regulation of immunoglobulin E class-switch recombination. Nat Rev Immunol. 2003;3(9):721–732. [PubMed: 12949496]
6. He JS, Narayanan S, Subramaniam S, Ho WQ, Lafaille JJ, Curotto de Lafaille MA. Biology of IgE production: IgE cell differentiation and the memory of IgE responses. Current topics in microbiology and immunology. 2015;388:1–19. [PubMed: 25553792]
7. Croote D, Darmanis S, Nadeau KC, Quake SR. High-affinity allergen-specific human antibodies cloned from single IgE B cell transcriptomes. Science. 2018;362(6420):1306–1309. [PubMed: 30545888]
8. Mita H, Yasueda H, Akiyama K. Affinity of IgE antibody to antigen influences allergen-induced histamine release. Clin Exp Allergy. 2000;30(11):1583–1589. [PubMed: 11069567]
9. Christensen LH, Holm J, Lund G, Riise E, Lund K. Several distinct properties of the IgE repertoire determine effector cell degranulation in response to allergen challenge. J Allergy Clin Immunol. 2008;122(2):298–304. [PubMed: 18572230]
10. Saunders SP, Ma EGM, Aranda CJ, Curotto de Lafaille MA. Non-classical B Cell Memory of Allergic IgE Responses. Front Immunol. 2019;10:715. [PubMed: 31105687]
11. Erazo A, Kutchukhidze N, Leung M, et al. Unique maturation program of the IgE response in vivo. Immunity. 2007;26(2):191–203. [PubMed: 17292640]
12. He JS, Meyer-Hermann M, Xiangying D, et al. The distinctive germinal center phase of IgE+ B lymphocytes limits their contribution to the classical memory response. J Exp Med. 2013;210(12):2755–2771. [PubMed: 24218137]
13. Yang Z, Sullivan BM, Allen CD. Fluorescent in vivo detection reveals that IgE(+) B cells are restrained by an intrinsic cell fate predisposition. Immunity. 2012;36(5):857–872. [PubMed: 22406270]
14. He JS, Subramaniam S, Narang V, et al. IgG1 memory B cells keep the memory of IgE responses. Nat Commun. 2017;8(1):641. [PubMed: 28935935]

15. Turqueti-Neves A, Otte M, Schwartz C, et al. The Extracellular Domains of IgG1 and T Cell-Derived IL-4/IL-13 Are Critical for the Polyclonal Memory IgE Response In Vivo. PLoS Biol. 2015;13(11):e1002290. [PubMed: 26523376]
16. Xiong H, Dolpady J, Wabl M, Curotto de Lafaille MA, Lafaille JJ. Sequential class switching is required for the generation of high affinity IgE antibodies. J Exp Med. 2012;209(2):353–364. [PubMed: 22249450]
17. Takhar P, Corrigan CJ, Smurthwaite L, et al. Class switch recombination to IgE in the bronchial mucosa of atopic and nonatopic patients with asthma. J Allergy Clin Immunol. 2007;119(1):213–218. [PubMed: 17208604]
18. Looney TJ, Lee JY, Roskin KM, et al. Human B-cell isotype switching origins of IgE. J Allergy Clin Immunol. 2016;137(2):579–586 e577. [PubMed: 26309181]
19. Bashford-Rogers RJM, Bergamaschi L, McKinney EF, et al. Analysis of the B cell receptor repertoire in six immune-mediated diseases. Nature. 2019;574(7776):122–126. [PubMed: 31554970]
20. Hofmaier S, Hatzler L, Rohrbach A, et al. "Default" versus "pre-atopic" IgG responses to foodborne and airborne pathogenesis-related group 10 protein molecules in birch-sensitized and nonatopic children. J Allergy Clin Immunol. 2015;135(5):1367–1374 e1361-1368. [PubMed: 25458000]
21. Schwarz A, Panetta V, Cappella A, et al. IgG and IgG4 to 91 allergenic molecules in early childhood by route of exposure and current and future IgE sensitization: Results from the Multicentre Allergy Study birth cohort. J Allergy Clin Immunol. 2016;138(5):1426–1433 e1412. [PubMed: 27264457]
22. Nelms K, Keegan AD, Zamorano J, Ryan JJ, Paul WE. The IL-4 receptor: signaling mechanisms and biologic functions. Annu Rev Immunol. 1999;17:701–738. [PubMed: 10358772]
23. McCormick SM, Heller NM. Commentary: IL-4 and IL-13 receptors and signaling. Cytokine. 2015;75(1):38–50. [PubMed: 26187331]
24. Rothman P, Lutzker S, Cook W, Coffman R, Alt FW. Mitogen plus interleukin 4 induction of C epsilon transcripts in B lymphoid cells. J Exp Med. 1988;168(6):2385–2389. [PubMed: 3264328]
25. Messner B, Stutz AM, Albrecht B, Peiritsch S, Woisetschlager M. Cooperation of binding sites for STAT6 and NF kappa B/rel in the IL-4-induced up-regulation of the human IgE germline promoter. J Immunol. 1997;159(7):3330–3337. [PubMed: 9317131]
26. Gascan H, Gauchat JF, Aversa G, Van Vlasselaer P, de Vries JE. Anti-CD40 monoclonal antibodies or CD4+ T cell clones and IL-4 induce IgG4 and IgE switching in purified human B cells via different signaling pathways. J Immunol. 1991;147(1):8–13. [PubMed: 1711085]
27. Zhang K, Clark EA, Saxon A. CD40 stimulation provides an IFN-gamma-independent and IL-4-dependent differentiation signal directly to human B cells for IgE production. J Immunol. 1991;146(6):1836–1842. [PubMed: 1706382]
28. Banchereau J, Bazan F, Blanchard D, et al. The CD40 antigen and its ligand. Annu Rev Immunol. 1994;12:881–922. [PubMed: 7516669]
29. Berberich I, Shu GL, Clark EA. Cross-linking CD40 on B cells rapidly activates nuclear factor-kappa B. J Immunol. 1994;153(10):4357–4366. [PubMed: 7525701]
30. Muramatsu M, Kinoshita K, Fagarasan S, Yamada S, Shinkai Y, Honjo T. Class switch recombination and hypermutation require activation-induced cytidine deaminase (AID), a potential RNA editing enzyme. Cell. 2000;102(5):553–563. [PubMed: 11007474]
31. Goenka S, Kaplan MH. Transcriptional regulation by STAT6. Immunol Res. 2011;50(1):87–96. [PubMed: 21442426]
32. Gordon J, Katira A, Strain AJ, Gillis S. Inhibition of interleukin 4-promoted CD23 production in human B lymphocytes by transforming growth factor-beta, interferons or anti-CD19 antibody is overriden on engaging CD40. Eur J Immunol. 1991;21(8):1917–1922. [PubMed: 1714394]
33. Muehlinghaus G, Cigliano L, Huehn S, et al. Regulation of CXCR3 and CXCR4 expression during terminal differentiation of memory B cells into plasma cells. Blood. 2005;105(10):3965–3971. [PubMed: 15687242]
34. Gauchat JF, Aversa G, Gascan H, de Vries JE. Modulation of IL-4 induced germline epsilon RNA synthesis in human B cells by tumor necrosis factor-alpha, anti-CD40 monoclonal antibodies

or transforming growth factor-beta correlates with levels of IgE production. Int Immunol. 1992;4(3):397–406. [PubMed: 1373645]

35. Ellebedy AH, Jackson KJ, Kissick HT, et al. Defining antigen-specific plasmablast and memory B cell subsets in human blood after viral infection or vaccination. Nat Immunol. 2016;17(10):1226–1234. [PubMed: 27525369]
36. Stewart A, Ng JC, Wallis G, Tsioligka V, Fraternali F, Dunn-Walters DK. Single-Cell Transcriptomic Analyses Define Distinct Peripheral B Cell Subsets and Discrete Development Pathways. Front Immunol. 2021;12:602539. [PubMed: 33815362]
37. Yoshihara Y, Ishiuji Y, Yoshizaki A, et al. IL-10-Producing Regulatory B Cells Are Decreased in Patients with Atopic Dermatitis. J Invest Dermatol. 2019;139(2):475–478. [PubMed: 30236612]
38. Ma S, Satitsuksanoa P, Jansen K, Cevhertas L, van de Veen W, Akdis M. B regulatory cells in allergy. Immunol Rev. 2021;299(1):10–30. [PubMed: 33345311]
39. Wu JQ, Seay M, Schulz VP, et al. Tcf7 is an important regulator of the switch of self-renewal and differentiation in a multipotential hematopoietic cell line. PLoS Genet. 2012;8(3):e1002565. [PubMed: 22412390]
40. Albrecht I, Niesner U, Janke M, et al. Persistence of effector memory Th1 cells is regulated by Hopx. Eur J Immunol. 2010;40(11):2993–3006. [PubMed: 21061432]
41. Cowling VH. Regulation of mRNA cap methylation. Biochem J. 2009;425(2):295–302. [PubMed: 20025612]
42. Draber P, Vonkova I, Stepanek O, et al. SCIMP, a transmembrane adaptor protein involved in major histocompatibility complex class II signaling. Mol Cell Biol. 2011;31(22):4550–4562. [PubMed: 21930792]
43. Cresswell P. Invariant chain structure and MHC class II function. Cell. 1996;84(4):505–507. [PubMed: 8598037]
44. Defrance T, Aubry JP, Rousset F, et al. Human recombinant interleukin 4 induces Fc epsilon receptors (CD23) on normal human B lymphocytes. J Exp Med. 1987;165(6):1459–1467. [PubMed: 2953844]
45. Gauchat JF, Lebman DA, Coffman RL, Gascan H, de Vries JE. Structure and expression of germline epsilon transcripts in human B cells induced by interleukin 4 to switch to IgE production. J Exp Med. 1990;172(2):463–473. [PubMed: 1695667]
46. Or R, Renz H, Terada N, Gelfand EW. Regulation of B-cell immune responses: predominant role of interleukin-4 in triggering cell proliferation and Ig production in competent B cells. Clin Immunol Immunopathol. 1994;72(1):141–149. [PubMed: 8020187]
47. Graber P, Gretener D, Herren S, et al. The distribution of IL-13 receptor alpha1 expression on B cells, T cells and monocytes and its regulation by IL-13 and IL-4. Eur J Immunol. 1998;28(12):4286–4298. [PubMed: 9862366]
48. de Vries JE, Punnonen J, Cocks BG, Aversa G. The role of T/B cell interactions and cytokines in the regulation of human IgE synthesis. Semin Immunol. 1993;5(6):431–439. [PubMed: 7510139]
49. Gowthaman U, Chen JS, Zhang B, et al. Identification of a T follicular helper cell subset that drives anaphylactic IgE. Science. 2019;365(6456).
50. Harris DP, Goodrich S, Gerth AJ, Peng SL, Lund FE. Regulation of IFN-gamma production by B effector 1 cells: essential roles for T-bet and the IFN-gamma receptor. J Immunol. 2005;174(11):6781–6790. [PubMed: 15905519]
51. Wang NS, McHeyzer-Williams LJ, Okitsu SL, Burris TP, Reiner SL, McHeyzer-Williams MG. Divergent transcriptional programming of class-specific B cell memory by T-bet and RORalpha. Nat Immunol. 2012;13(6):604–611. [PubMed: 22561605]
52. Zumaquero E, Stone SL, Scharer CD, et al. IFNgamma induces epigenetic programming of human T-bet(hi) B cells and promotes TLR7/8 and IL-21 induced differentiation. Elife. 2019;8.
53. Frisullo G, Nociti V, Iorio R, et al. Increased expression of T-bet in circulating B cells from a patient with multiple sclerosis and celiac disease. Hum Immunol. 2008;69(12):837–839. [PubMed: 18940217]
54. Rubtsov AV, Rubtsova K, Fischer A, et al. Toll-like receptor 7 (TLR7)-driven accumulation of a novel CD11c(+) B-cell population is important for the development of autoimmunity. Blood. 2011;118(5):1305–1315. [PubMed: 21543762]

55. Rubtsova K, Marrack P, Rubtsov AV. TLR7, IFNgamma, and T-bet: their roles in the development of ABCs in female-biased autoimmunity. Cell Immunol. 2015;294(2):80–83. [PubMed: 25541140]

56. Obeng-Adjei N, Portugal S, Holla P, et al. Malaria-induced interferon-gamma drives the expansion of Tbethi atypical memory B cells. PLoS Pathog. 2017;13(9):e1006576. [PubMed: 28953967]

57. Bagnara D, Squillario M, Kipling D, et al. A Reassessment of IgM Memory Subsets in Humans. J Immunol. 2015;195(8):3716–3724. [PubMed: 26355154]

58. Seifert M, Kuppers R. Human memory B cells. Leukemia. 2016;30(12):2283–2292. [PubMed: 27499139]

59. Le Floc'h A, Allinne J, Nagashima K, et al. Dual blockade of IL-4 and IL-13 with dupilumab, an IL-4Ralpha antibody, is required to broadly inhibit type 2 inflammation. Allergy. 2020;75(5):1188–1204. [PubMed: 31838750]

60. Bruton K, Spill P, Vohra S, et al. Interrupting reactivation of immunologic memory diverts the allergic response and prevents anaphylaxis. J Allergy Clin Immunol. 2021;147(4):1381–1392. [PubMed: 33338539]

61. Castro M, Corren J, Pavord ID, et al. Dupilumab Efficacy and Safety in Moderate-to-Severe Uncontrolled Asthma. N Engl J Med. 2018;378(26):2486–2496. [PubMed: 29782217]

62. Beck LA, Thaci D, Hamilton JD, et al. Dupilumab treatment in adults with moderate-to-severe atopic dermatitis. N Engl J Med. 2014;371(2):130–139. [PubMed: 25006719]

63. Wenzel S, Ford L, Pearlman D, et al. Dupilumab in persistent asthma with elevated eosinophil levels. N Engl J Med. 2013;368(26):2455–2466. [PubMed: 23688323]

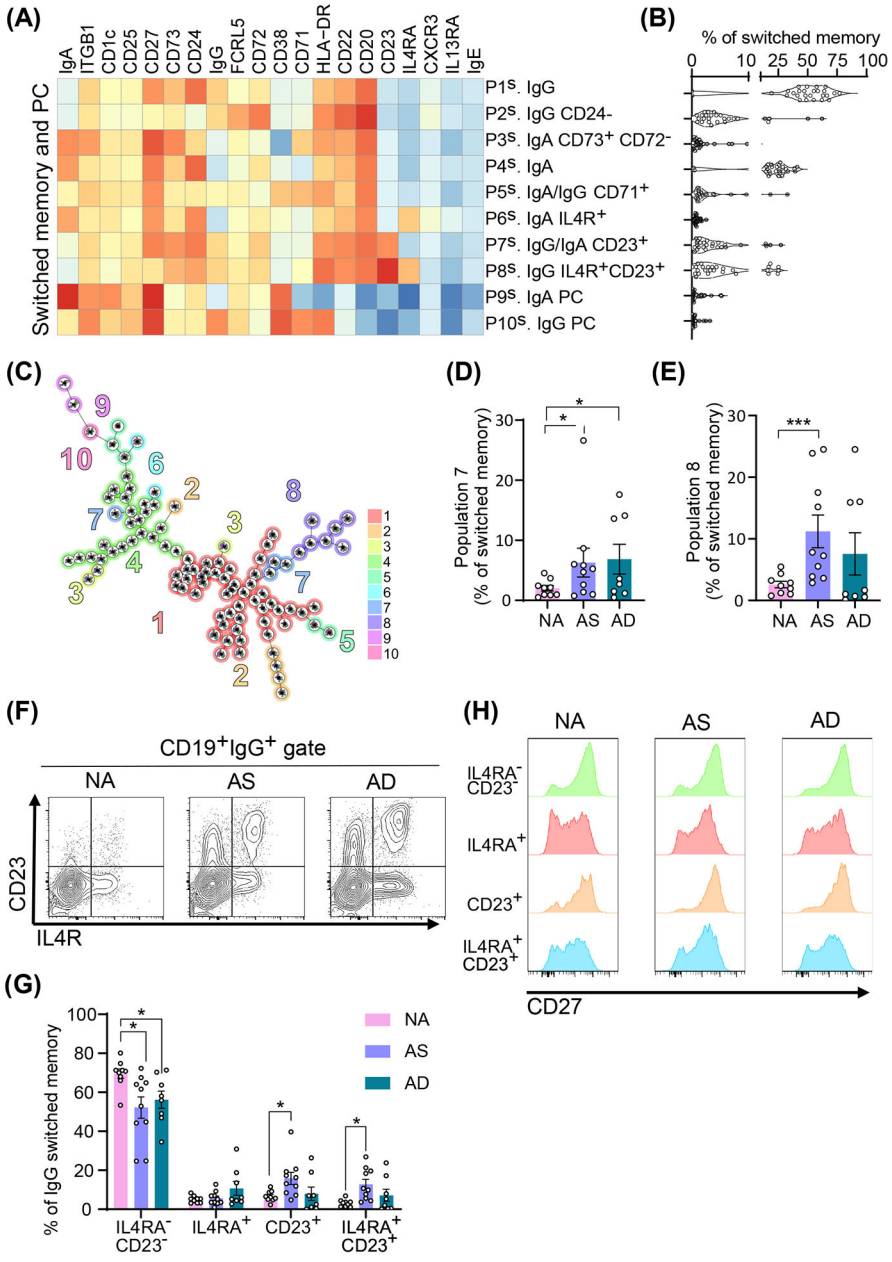

FIGURE 1.

Full spectral flow cytometry analysis of switched memory B cells and plasma cells from atopic and non-atopic subjects. (A-E) Unsupervised analysis of $IgM^{-}IgD^{-}CD19^{+}$ B cells from concatenated samples using the FlowSOM algorithm. (A) The heatmap on the left shows the relative expression levels of the analyzed listed proteins (x-axis, top) and (B) the identification of populations (y-axis, right). The populations' composition in all samples is shown in the violin plots on the right. (C) Tree of clusters showing the same populations as in A. Populations $P7^{S}$ and $P8^{S}$ branch from the largest population $P1^{S}$, containing IgG memory cells. (D-E) Frequency of populations $P7^{S}$ (C) and $P8^{S}$ (D) in non-atopic (NA), asthma (AS), and atopic dermatitis (AD) subjects. (F-H) Conventional gating analysis of CD23 and IL4R expression in IgG memory B cells. (F) Representative flow plots. (G)

Percentages of $IL4R^{-}CD23^{-}$, $IL4R^{+}$, $CD23^{+}$, and $IL4R^{+}CD23^{+}$ in IgG memory cells from samples of NA, AS, and AD subjects. (H) Representative histograms of CD27 expression in $IL4R^{-}CD23^{-}$, $IL4R^{+}$, $CD23^{+}$, and $IL4R^{+}CD23^{+}$ IgG memory cells. *: $P<0.05$; ***: $P<0.001$.

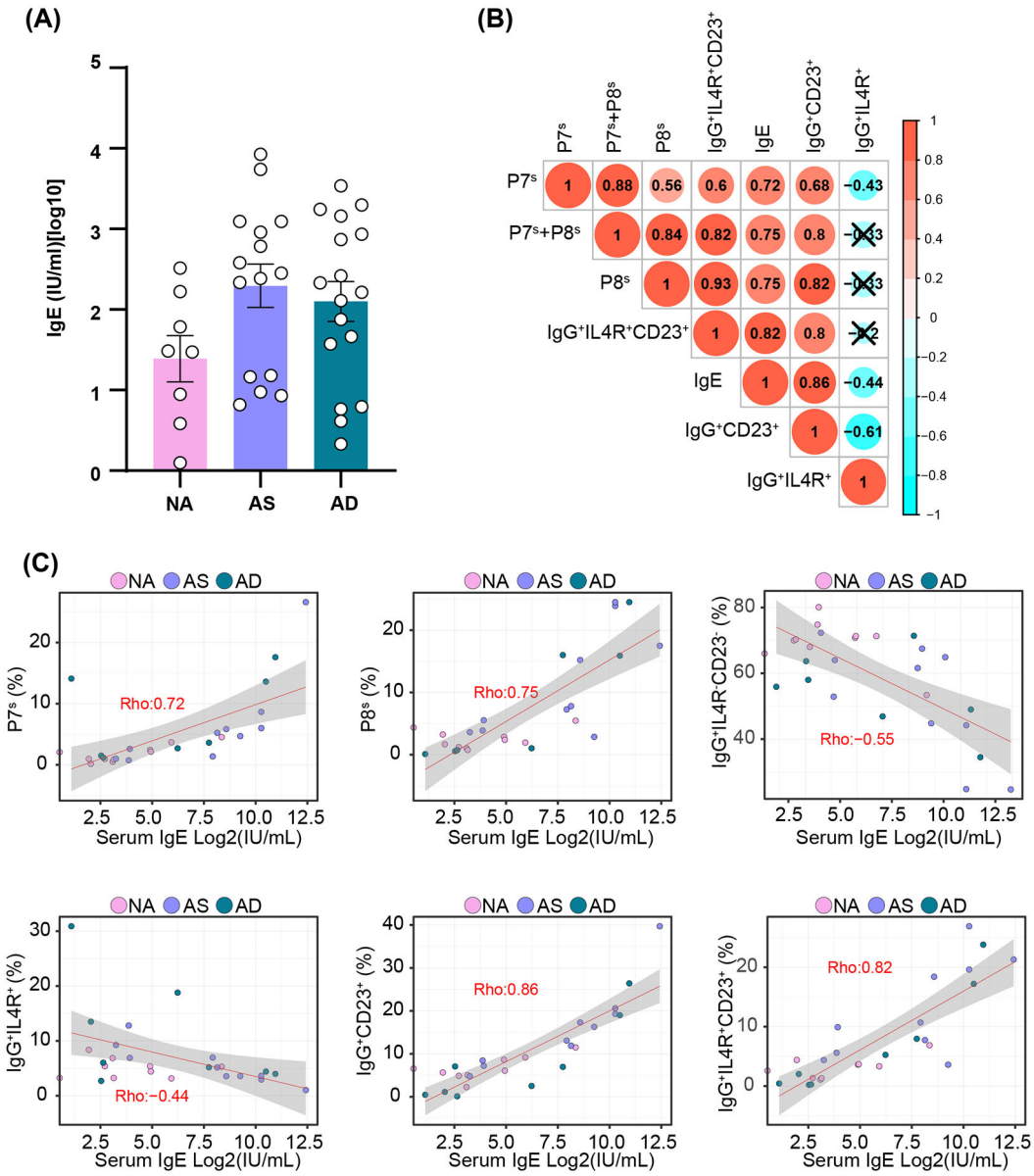

FIGURE 2.

IL4R$^+$CD23$^+$ and CD23$^+$ IgG$^+$ MBC frequencies correlate with plasma levels of IgE. (A) IgE levels among non-atopic (NA), asthma (AS), and atopic dermatitis (AD) subjects. (B) Spearman correlation matrix between: CD23 and IL4R expressing switched memory populations defined by unsupervised analysis (P7^S and P8^S), IgG memory populations defined by conventional gating (IL4R$^-$CD23$^-$, IL4R$^+$, CD23$^+$, IL4R$^+$CD23$^+$, and all CD23$^+$/IL4R$^+$), and levels of total IgE in plasma. An X indicates non-significant correlation (P>0.05) (C) Scatterplots showing all individual sample correlations between the switched memory populations of interest (as in B), and plasma IgE levels.

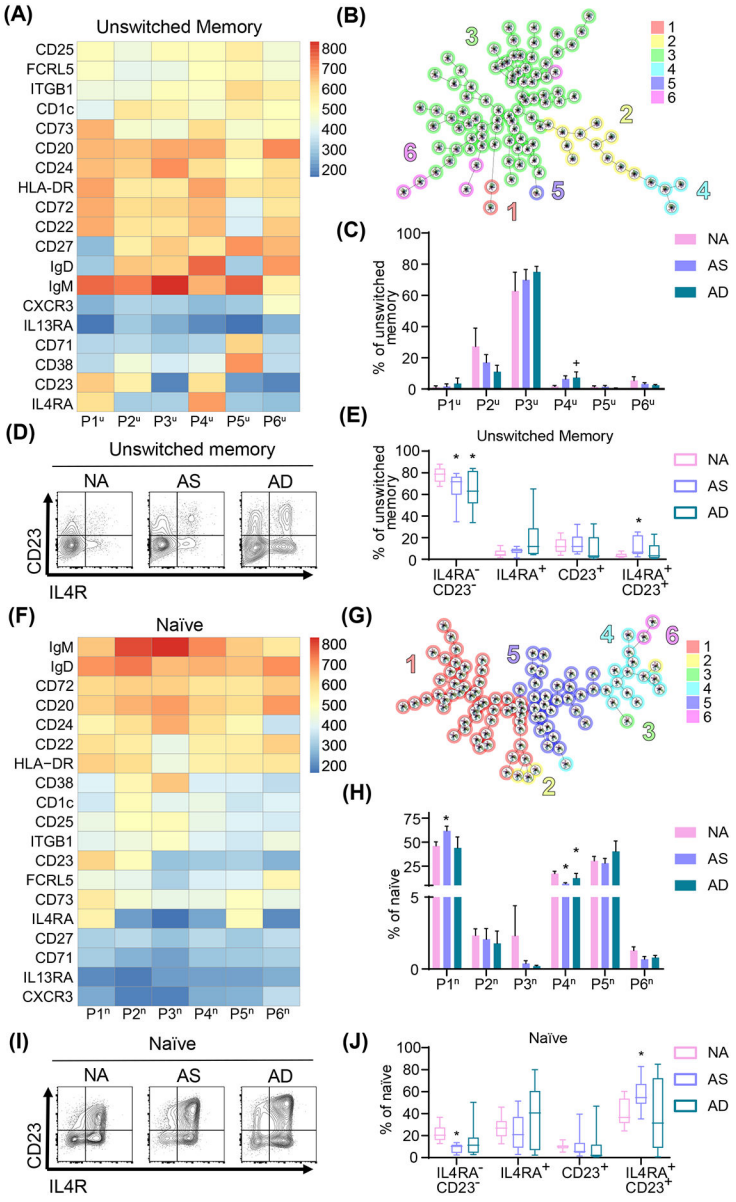

FIGURE 3.

Full spectral flow cytometry analysis of unswitched memory B cells and naïve B cells from atopic and non-atopic subjects. (A-C) Unsupervised analysis of IgM^+ and/or IgD^+ $CD27^+$ $CD19^+$ B cells from concatenated samples using the FlowSOM algorithm. (A) Heatmap showing the relative expression levels of the analyzed listed proteins (y-axis, left) and the identification of populations (x-axis, bottom). (B) Tree of clusters showing the same populations as in A. (C) Frequency of the different populations $P1^u$-$P6^u$ in non-atopic (NA), asthma (AS), and atopic dermatitis (AD) subjects. (D-E) Conventional gating analysis of CD23 and IL4R expression in unswitched memory B cells. (D) Representative flow plots. (E) Percentages of $IL4R^-CD23^-$, $IL4R^+$, $CD23^+$, and $IL4R^+CD23^+$ in unswitched memory B cells from samples of NA, AS, and AD subjects. (F-H) Unsupervised analysis of IgM^+ and/or IgD^+ $CD27^-$ $CD19^+$ B cells from concatenated samples using the FlowSOM

algorithm. (F) Heatmap showing the relative expression levels of the analyzed listed proteins (y-axis, left) and the identification of populations (x-axis, bottom). (G) Tree of clusters showing the same populations as in F. (H) Frequency of the different populations $P1^N$-$P6^N$ in non-atopic (NA), asthma (AS), and atopic dermatitis (AD) subjects. (I-J) Conventional gating analysis of CD23 and IL4R expression in naïve B cells. (I) Representative flow plots. (J) Percentage of $IL4R^-CD23^-$, $IL4R^+$, $CD23^+$, and $IL4R^+CD23^+$ in naïve B cells from samples of NA, AS and AD subjects. $^+$: $P<0.1$; *: $P<0.05$.

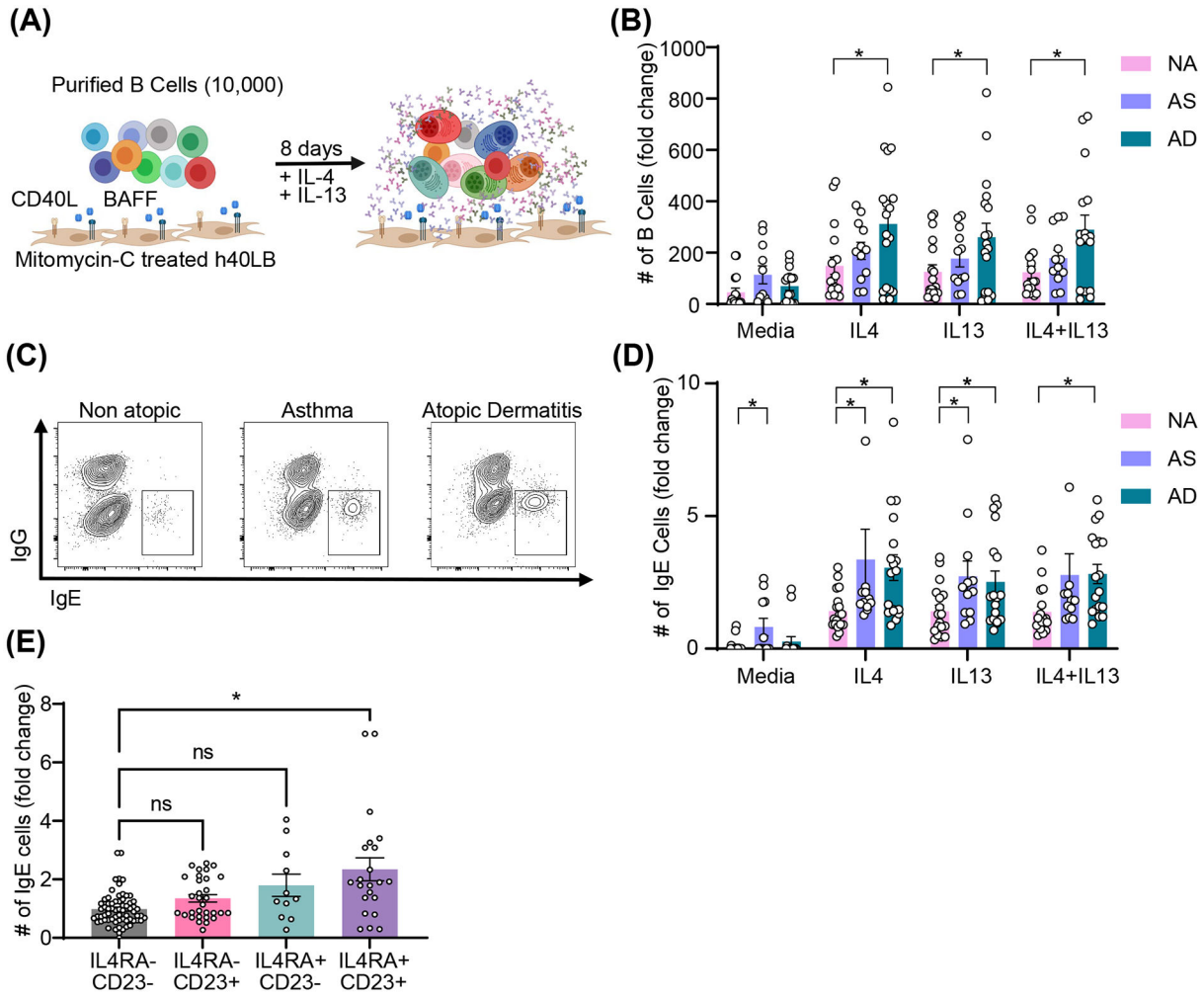

FIGURE 4.

B lymphocytes from atopic subjects have a high propensity to switch to IgE. (A) Schematic representation of the ex vivo system for culturing B cells. (B) Number of total B cells after 8 days of culture without added cytokines (medium) or with IL-4, IL-13, or IL-4+IL-13. (C) Representative plots showing IgE cells after 8 days in cultures with IL-4. (D) Number of IgE cells after 8 days without added cytokines (medium) or with IL-4, IL-13, or IL-4+IL-13. (E) Number of IgE cells after 8 days of in vitro culture of sorted IgG cells expressing $IL4R^{-}CD23^{-}$, $IL4R^{+}CD23^{-}$, $IL4R^{-}CD23^{+}$, and $IL4R^{+}CD23^{+}$. Cells were cultured as in A with IL-4. *: $P<0.05$: ns= non-significant.

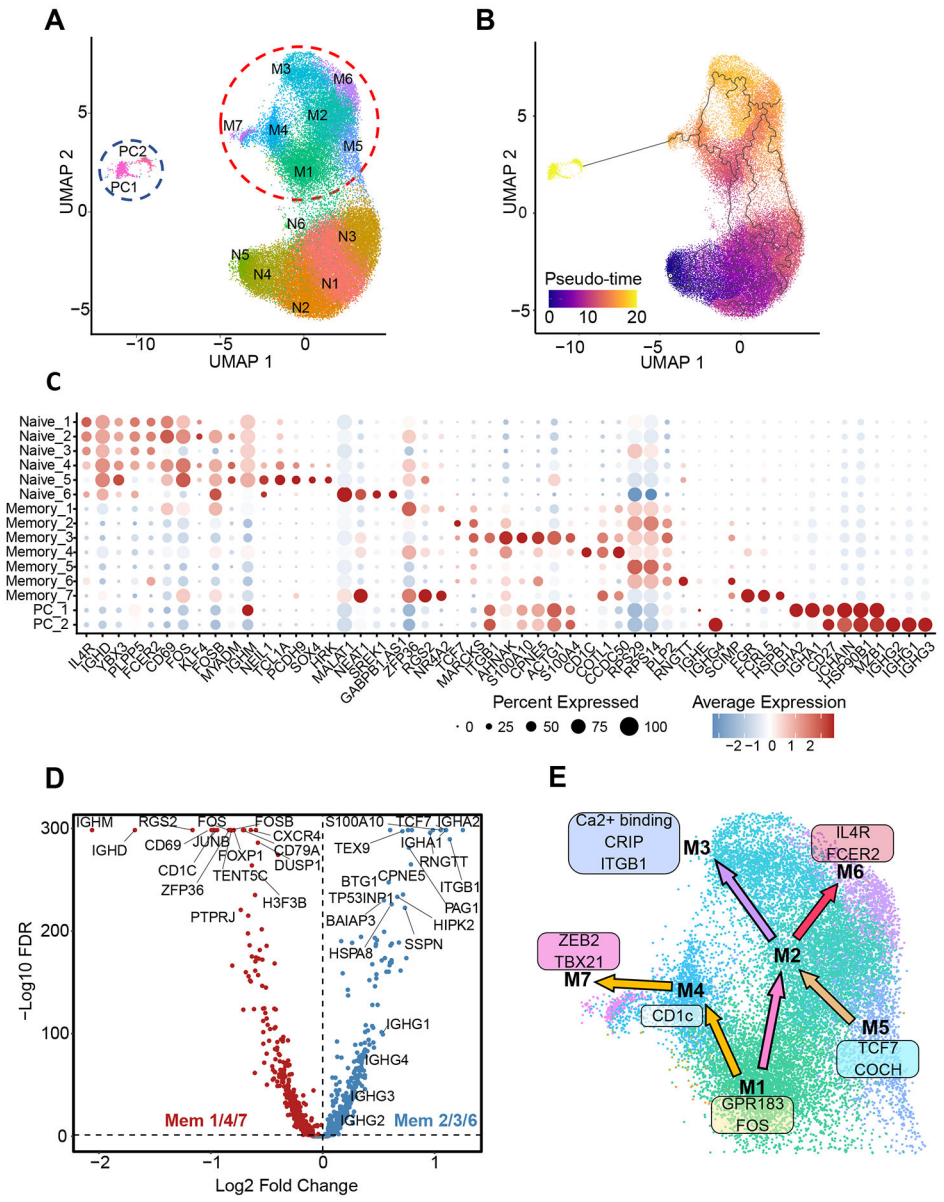

FIGURE 5.

Transcriptional profile of B lymphocytes from atopic and non-atopic subjects. (A) UMAP representation of 15 B cell clusters after single-cell sequencing, post quality control, and data integration with SeuratV4. Naïve B cell clusters are represented by N, while Memory B cells with M and plasma with PC. Circles encompass these 3 cell sub-types and the colors are unique per cluster. (B) UMAP representation colored by pseudotime based on Monocle3 unsupervised graph and pseudotime analysis. The starting point was defined as naïve cluster 5 and the endpoint was plasma cells. The graph shows as lines the most associated cells based on their gene expression, highlighting two potential routes for naïve cells and memory cells. (C) Differential expression results show the top genes per cell cluster. The colors indicate the fold change in average expression, while the size shows the percent of cells expressing each marker. (D) Volcano plot showing the differential

expression results between Memory B cells clusters 1,4,7 against 2,3 and 6. (E) Schematic representation of the two possible groups of Memory B Cells based on our dataset. Two possible paths of differentiation identified by pseudotime, M1-M4-M7 and M5-M2-M3-M6 are shown. Representative differentially expressed genes for the paths and the individual memory clusters are shown.

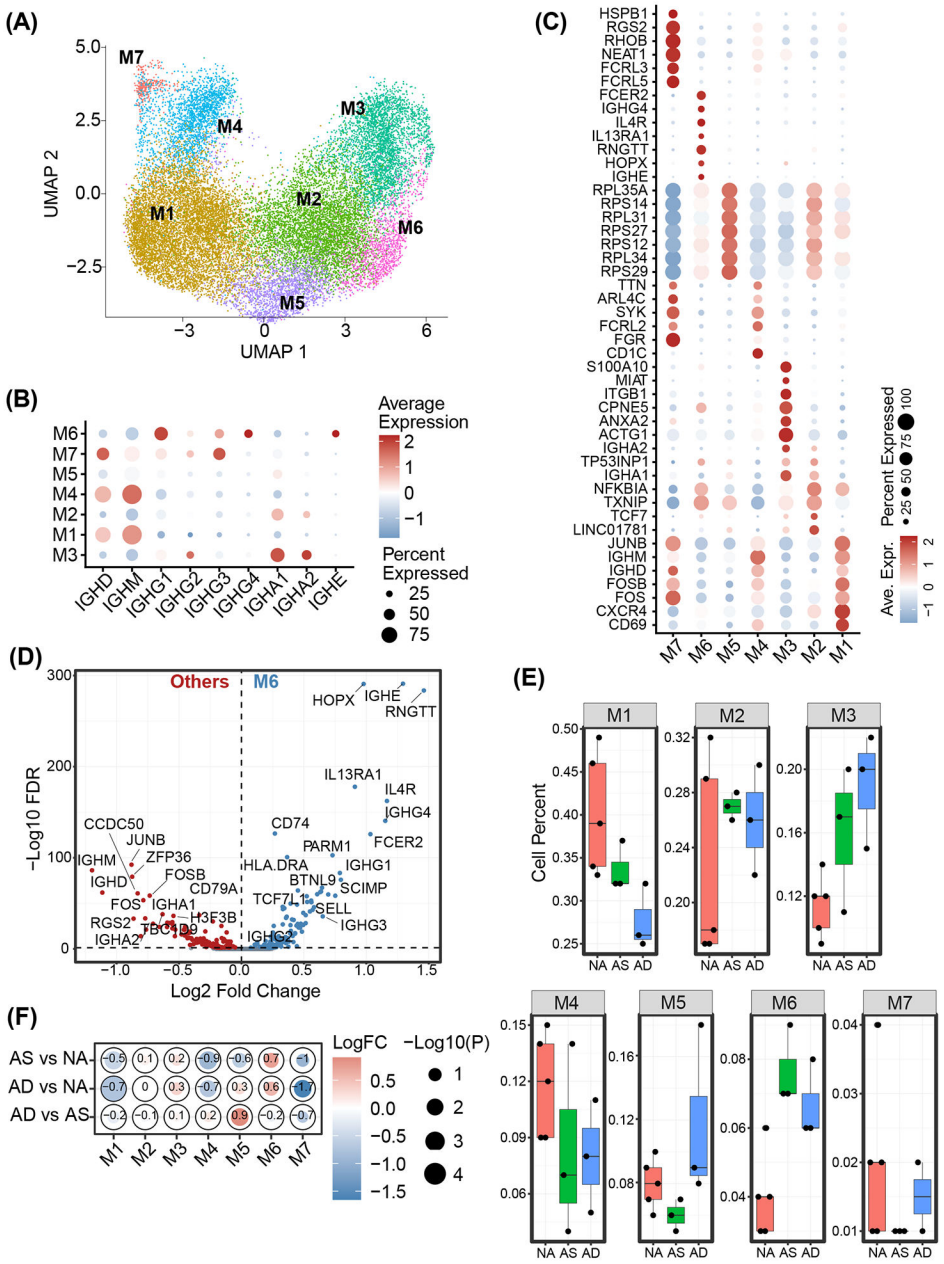

FIGURE 6.

Identification of a memory cluster with type 2 immune marks. (A) UMAP representation of memory B cells after re-clustering without naïve and plasma cells. (B) Dotplot showing the expression of immunoglobulin heavy chains per cluster. The circle's color indicates the average expression of cluster cells represented as the fold change relative to all clusters, while the size indicates the percent of cells expressing each marker. (C) Heatmap showing the top markers per memory B cell cluster and the difference in expression between each cluster and the average expression of all cells. (D) Differential abundance analysis showing the log2 fold change between comparisons between groups (AS, AD, and NA). (E) Boxplots showing the percent cluster distribution of cells from each subject. sample grouped based on

their clinical characteristics (NA=Non-Atopic, AS=Asthmatic, and AD=Atopic-Dermatitis). (F) Differential abundance analysis of the comparisons between NA, AD, and AS (Y-axis). The difference in log2 fold change is shown in color, while significance is shown as size or −Log10 (P.value).